

PAPER

Quench transient current and quench propagation limit in pancake wound REBCO coils as a function of contact resistance, critical current, and coil size

To cite this article: W Denis Markiewicz *et al* 2019 *Supercond. Sci. Technol.* **32** 105010

View the [article online](#) for updates and enhancements.

Recent citations

- [Design and Performance Estimation of a 20 T 46 mm No-Insulation All-REBCO User Magnet](#)
Kwangmin Kim *et al*
- [Contact resistivity due to oxide layers between two REBCO tapes](#)
Jun Lu *et al*



IOP | ebooks™

Bringing together innovative digital publishing with leading authors from the global scientific community.

Start exploring the collection—download the first chapter of every title for free.

Quench transient current and quench propagation limit in pancake wound REBCO coils as a function of contact resistance, critical current, and coil size

W Denis Markiewicz¹ , Thomas Painter, Iain Dixon and Mark Bird

National High Magnetic Field Laboratory, 1800 E. Paul Dirac Dr, Tallahassee FL 32310, United States of America

E-mail: markwcz@magnet.fsu.edu

Received 2 March 2019, revised 21 May 2019

Accepted for publication 5 July 2019

Published 12 September 2019



Abstract

It is a general belief that no insulation (NI) coil technology is a path to very high field superconducting coils. Recent experience has shown that there are aspects of NI coil design that, if not addressed, can possibly lead to coil failures. One potential problem area is the large transient currents that are associated with quench propagation in NI coils. In an attempt to understand and possibly find ways to minimize the potential for damage from quench transients, a parameter study was undertaken to examine the factors that influence the magnitude of transient currents during quench in NI coils. The characteristics of the transient currents are first examined. A study is then made of a set of test coils, looking at quench propagation and the transient current magnitude as a function of contact resistance, critical current, and importantly coil size. For each coil size, it is found that as the contact resistance increases, the magnitude of quench transient currents is reduced until a condition where effective quench propagation ceases, called the quench propagation limit (QPL). As the QPL is approached, the amplitude of the transient current is decreased and may provide a regime where quench induced stress can be effectively contained in coil designs. As coil size increases, the value of contact resistance associated with the limit of quench propagation increases as well. At large coil sizes that will be characteristic of high field REBCO magnets, the QPL extends to truly large values of contact resistance compared to values observed between bare conductors. The use of methods such as resistive films on conductors and co-wind steel will be required to increase contact resistance. In recognition of this development, the use of high contact resistance achieved in this manner is appropriately called resistive insulation coil technology.

Keywords: REBCO, no insulation NI coils, quench, contact resistance, resistive insulation

(Some figures may appear in colour only in the online journal)

1. Introduction

The initial motivation for REBCO ($\text{REBa}_2\text{Cu}_3\text{O}_{7-\delta}$, RE = Rare Earth) no insulation (NI) coils, beyond dealing with the lack of a good insulation, was to increase the mechanical properties by removal of soft insulation, and simultaneously increase the

current density. Subsequently, small NI coils were shown to exhibit high stability and importantly, to be self-protecting [1–3]. Further development showed that increasingly large coils exhibited rapid quench propagation and again self-protection [4]. In a fundamental paper, the underlying quench propagation mechanism was shown in detail to be a dynamic inductive process as opposed to the essentially thermal diffusion mechanism familiar with low temperature superconductors. Rapid

¹ Author to whom any correspondence should be addressed.

quench propagation was found to be associated with large transient currents of both the azimuthal current and an equally large reverse radial current that was identified as the source of the heating that drives the quench [5]. As the technology has progressed, larger NI coils have been constructed. There has been demonstration of the potential of NI coils in achieving high field at high current density [6]. There have also been reports of damage to significant NI coils that either was the cause of quench or was the result of quench [7–9]. There could be a number of contributing reasons for coil quench and damage, including conventional aspects of coil design and construction, but the experience of these coils is an indication that NI coils are not immune to potential problems during quench.

There is increasing awareness that mechanical design is of paramount importance in high field REBCO coils, and that robust mechanical design is an aspect of quench protection design [10, 11]. During quench there are transient currents that go beyond the currents associated with normal operation, and there are corresponding forces that go beyond the forces associated with normal operation. An understanding of the quench transient currents is required to properly account for those currents and forces in the mechanical design. Large transients in the azimuthal current will result in large transient forces and stress in the hoop direction of the windings. Equally large transients during quench in the radial direction will result in a torque distributed within and between disks. Another source of mechanical force during quench in REBCO NI coils appears in multiple coil magnets. The nature of quench in NI coils results in a change in current flow from the azimuthal to the radial direction and a change in the electrical nature of the windings from inductive to resistive. As the quench front moves through a coil, the current at a given location shifts from being azimuthal prior to the arrival of the quench front, to radial after passage of the quench front. In this way, the inductive center of a coil shifts in the axial direction following the quench propagation and results, in a multiple coil magnet, in an axial offset magnetic force between the coils.

In this paper, the primary focus is on large azimuthal transient currents associated with quench and by implication the forces associated with those currents. There is no explicit focus on torque, but there is a direct relation between the azimuthal transient currents and the radial transient currents. Those aspects of a design which tend to decrease the azimuthal transient currents also decrease the radial transients. The hoop direction and torque force components are therefore reduced in proportion. The present parameter study is made with a set of test coils in a background field magnet. Large axial forces result from quench of the test coils, but these forces are not necessarily indicative of axial quench forces in a fully designed multiple coil magnet in which care was taken to address axial forces. Therefore, axial forces are not reported in the present work.

The transient currents of the present work are to be distinguished from the usual concept of screening currents, which are induced in REBCO tape conductor during ramping of a coil and influence the central field value and the field uniformity, and are therefore of particular interest for REBCO NMR magnets [12, 13]. By nature, screening currents form persistent current loops in the conductor and result in a non-uniform

distribution of current across the conductor width. In the combined axial and radial field at the ends of a coil, the non-uniform current distribution of the screening currents results in a twisting torque which tends to stretch the far axial edge of the conductor, resulting in mechanical loading in addition to the hoop stress [14]. Evidence of damage and plastic yielding on the far edge of conductors has been observed recently in inspection of conductors from damaged coils. This observation has led to the suggestion that screening current effects are responsible for the observed conductor damage [9].

Screening currents, in the usual sense, are not included in the present analysis. There is no analysis of the distribution of currents across the width of the conductor. Rather, the analysis concerns the transient currents during quench. These are not typical screening currents which form a superconducting loop within the conductor, nor are the transient currents accurately described as transport currents. In the model of quench in NI coils, the excess transient current, above the transport current, is a large azimuthal current that returns back as a radial current through the turn to turn contact resistance. The transient current is therefore a loop current, similar to a screening current, but in a loop circuit that contains radial current and significant resistance. A more detailed quench analysis could additionally include the distribution of the current across the width of the conductor, and therefore the true shielding current effect, in addition to the transient current effects studied here.

2. Analysis method and test coil definition

The electromagnetic analysis of NI coil windings has, since the beginning, employed a number of circuit parameter models. In the initial lumped circuit model, the entire coil was modeled as a single inductor with parallel shunt resistor to simulate turn-to-turn contact resistance, while the superconductor to normal transition was incorporated as a variable resistor in series with the inductor [1]. The various refinements to the circuit model can be distinguished by the portion of the windings that is modeled by each inductor in the circuit. Thus, in a distributed lumped circuit model, each pancake or double pancake is modeled by a separate inductor [15]. In a further refinement, the axisymmetric distributed circuit model divides each pancake into a number of rings or radial sections, and each radial section is modeled as a separate inductor [5]. Finally, distributed circuit models are employed that further divide the radial sections into a number of circumferential arcs, with each arc segment being modeled as a separate inductor [16]. The present analysis is done with an axisymmetric distributed circuit model. The pancakes are divided radially into a number of sections of equal thickness and the pancake structure gives a natural division in the axial direction. There results a two dimensional grid in r and z of coil sections, with each section modeled by an LR circuit after the original lumped circuit model. The inductance of each section is mutually coupled throughout the coil. The shunt resistance of each section is computed from the contact resistance for the number of turns in the coil section. The contact resistance is assumed to be independent of

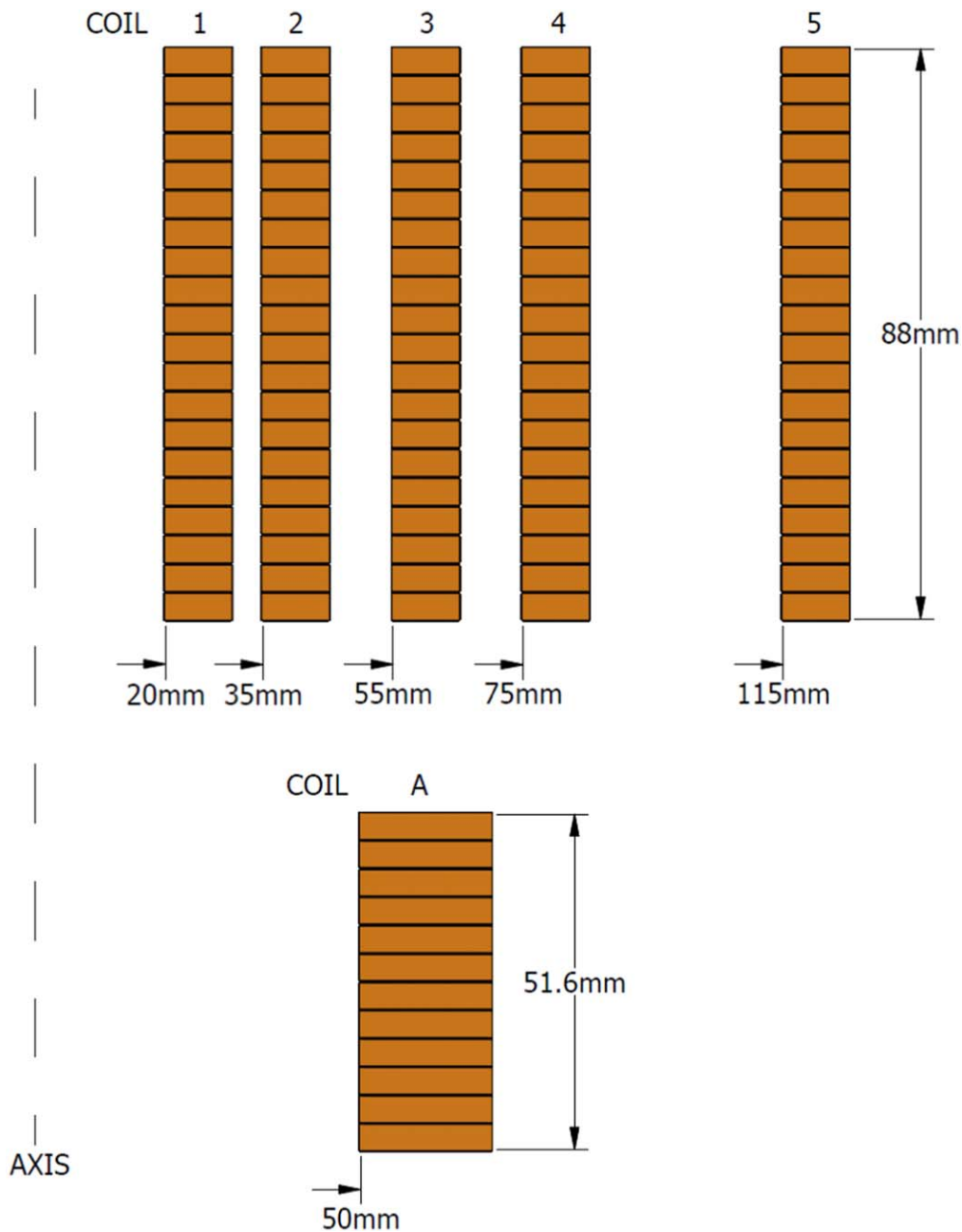


Figure 1. Cross sectional view of the pancake wound analysis test coils, which are operated individually in a nominal 30 T background field. Background field coil is not shown.

temperature in this analysis. At each time interval, the superconductor normal transition resistance is computed from the superconductor voltage per unit length given by

$$V_{pl} = V_0 \left(\frac{I_\theta}{I_c(B, \theta, T)} \right)^n, \quad (1)$$

where V_0 is the critical current criterion of $1 \mu\text{V cm}^{-1}$, I_θ is the circumferential current, $I_c(B, \theta, T)$ is the critical current as a function of field, field angle, and temperature, and where a value of 25 is assumed for the n -value n . At each time interval, the Kirchhoff equations for all the coupled coil sections are solved for the time derivatives of the circumferential currents, which together with the time increment gives

the new current values. The power in the circuits is computed and the temperature in each section is revised using temperature dependent materials properties. The critical current is adjusted according to the revised temperature and computed field. The quench analysis method is essentially that described previously [5].

The test coil cross sections are shown in figure 1 and test coil parameters in table 1. Initial results were obtained for quench transients in coil A, which is characterized by having 12 disks and a 20 mm winding depth. The majority of the analysis is done for a set of test coils 1–5, which are distinguished by having 20 disks and a 10 mm winding depth. In each case, the number of radial divisions N_r of the winding depth is such as to give a thickness of 1 mm to each radial

Table 1. Parameters of test coil A with 20 mm winding depth and 12 disks, and test coils 1–5 with 10 mm winding depth and 20 disks of increasing diameter.

	Units	Coil A	Coil 1	Coil 2	Coil 3	Coil 4	Coil 5
Inside radius a1	mm	50	20	35	55	75	115
Outside radius a2	mm	70	30	45	65	85	125
Coil length	mm	51.6	88	88	88	88	88
Number of disks		12	20	20	20	20	20
Radial sections		20	10	10	10	10	10
Operating current	A	250	250	250	250	250	250
Field increment	T	6.11	5.91	5.03	4.02	3.28	2.34
Outer field	T	28.16	30	30	30	30	30
Total field	T	34.27	35.91	35.03	34.02	33.28	32.34

section. The calculation time increment used for coil A was 0.1 μs , with output at 10 μs intervals, while the calculation time increment used for coils 1–5 was 1.0 μs with output at 100 μs intervals. The winding pack design for the test coils is shown in table 2. For all coils, the conductor has 40 μm total copper thickness and a limited thickness of co-wind reinforcement, none for coil A and 10 μm for coils 1–5. The details of the large outer coils used with coil A and with coils 1–5 are not essential to the analysis beyond providing the nominal 30 T background field and large series inductance. All coils operate at an initial current of 250 A.

3. Surface resistivity, contact resistance, and turn resistance

Contact resistance R_s is a fundamental quantity for NI coils and has been examined in some detail. Contact resistance between conductors has been shown to depend on surface preparation, on pressure and on pressure cycling [17, 18]. The contact resistance between turns is found to be strongly influenced by the presence of steel co-wind, which in NI coil technology is referred to as metallic insulation [19]. Contact resistance is recognized as originating from a combination of factors such as surface roughness and hardness, and a contribution from any resistive layer on the conductor or co-wind such as an oxide. The term metallic insulation is used to indicate the presence of steel co-wind, but it is recognized that the resistance associated with the co-wind is not attributable to the bulk metal resistivity, but rather comes primarily from the contact resistance factors including especially a resistive oxide (non-metallic) layer. In this regard, the term metallic insulation is something of a misnomer.

There has begun to be active attempts to adjust and control the value of the contact resistance, through the application of resistive films on the conductor, including copper oxide, and creation of oxide layers on steel co-wind by heat treatment in air [20, 21]. It is not the purpose of the present work to examine the engineering of the value of R_s . Rather, in order to examine the consequences for quench, the contact resistance is treated as a parameter with a broad range of possible values, but with a constant value for a particular coil design.

Table 2. Conductor and winding pack parameters for test coils A and 1–5.

	Units	WP A	WP 1–5
Copper thickness	μm	40	40
Hastelloy thickness	μm	50	50
Conductor thickness	μm	95	95
Co-wind thickness	μm	0	10
Turn thickness	μm	95	105
Conductor width	mm	4	4.1
Axial insulation thickness	mm	0.3	0.3
Copper current density	A mm^{-2}	1562	1524
Conductor current density	A mm^{-2}	658	642
Turn current density	A mm^{-2}	658	581
Average current density	A mm^{-2}	612	541

Contact resistance as used in the technology of NI coils is a resistance per unit area of contact between turns, and is therefore a surface resistivity. The terminology of contact resistance is widely used in the literature of NI coils and will be maintained here. In recognition of the surface resistivity nature, the contact resistance will be designated by the quantity R_s and interchangeably referred to as the surface resistivity.

A related quantity is the turn-to-turn resistance R_t , given by the ratio of R_s over the area between turns. It is noted that for a constant contact resistance or surface resistivity, the value of R_t varies through a coil according to the diameter of the turn. With the emphasis on contact resistance it is easily overlooked that, for the same value of contact resistance, small diameter coils have larger values of R_t than large diameter coils.

4. Quench transient current characteristics

After the onset of quench at one end of an NI coil, quench proceeds through the length of the coil by a large transient disturbance of the azimuthal current which is propagated by a process of mutual inductance, both within a disk and from disk to disk through the coil [5]. As an example of the quench transient current as seen in a given disk, for a quench initiated at the end of coil A, the quench transient current that occurs in

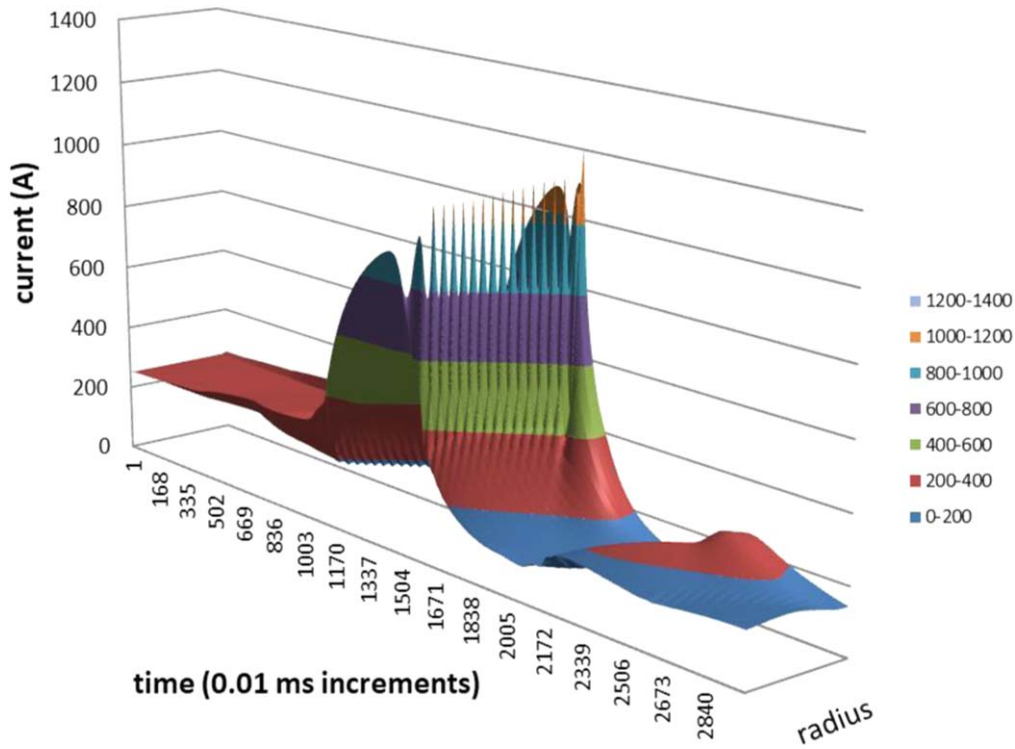


Figure 2. Quench transient current as a function of time in disk 7 of test coil A, shown through the radial depth of the coil from inside to outside radius, with a complex fast current peak. The line of sharp current spikes is the representation of a radial transient current wave in the calculation model with discrete radial sections.

disk 7 is shown in figure 2 as function of time through the radial depth of the disk. Initially, the current is the operating current of the coil. As the quench front reaches the disk, the current increase and decrease in time is abrupt. The distribution of current radially is not entirely uniform even in this relatively thin coil, but rather shows characteristic features. The coil is divided into a number of radial sections for calculation. The radial sections on the inner and outer surface of the coil experience a broader transient in time, probably due to inductive coupling effects. Between the inner and outer sections, figure 2 shows a fast radial propagation of the transient current through the radial depth of the coil. The current spikes seen along the crest of the transient current are the result of the discrete nature of the axisymmetric distributed circuit model and the presence of a finite propagation velocity in the radial direction. Another representation of the transient current in disk 7 of coil A is given in figure 3 where the current in four adjacent radial sections near the center of disk 7 is shown as a function of time in high resolution. The radial separation of the sections is 1 mm. The displacement in time of the peak current in each trace is a measure of the radial propagation velocity. If the radial depth of the sections, and therefore the separation of the sections, were to be decreased, the time displacement between peaks would be expected to decrease in proportion and in the limit would display a continuous wave of radial propagation.

Details of the disk to disk quench propagation through coil A in time are shown in figure 4, where the azimuthal transient currents are shown for each disk at a point approximately midway through the radial depth. Due to an

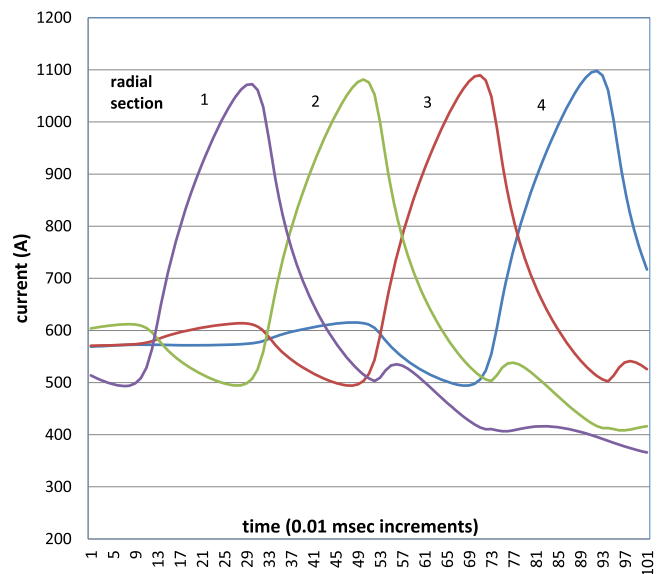


Figure 3. Quench transient current as a function of time in four adjacent radial sections near the center of disk 7 in coil A. The shift of the peak current in time from section to section is a measure of the radial propagation velocity of the quench. The small oscillations in each current trace are an inductive reaction to the radial advance of the current peak, followed by decrease in current after the peak and quench.

initial imposed condition of low critical current, quench is initiated in disk 1 which shows a resistive decrease in current. All subsequent disks show inductive current increase before quench. Here, at a contact resistance of $1.0 \text{ m}\Omega \text{ cm}^2$, the

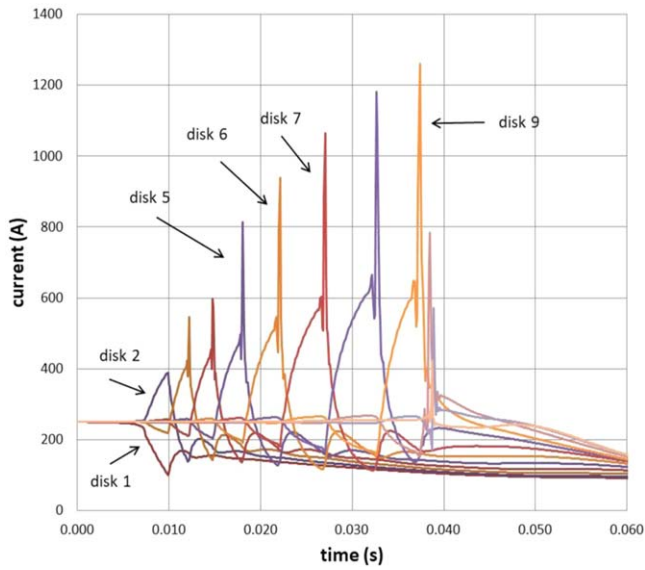


Figure 4. Progression of quench in time from disk to disk through coil A is seen in the transient currents at a fixed radius within the coil for R_s 1.0 $m\Omega\text{ cm}^2$. Initiation of quench in disk 1 shows a resistive trace with decreasing current, while subsequent disks in turn show an inductive increase in current and then quench.

transient currents in each disk appear to have two parts, one part being the lower, wider, longer duration part, and the other part being the upper very short duration large amplitude spike. The broad base of the transient may well reflect an average quench behavior of the disks, while the sharp peak may be the result of radial quench propagation within the disk.

It is interesting to see a comparison between the critical current (I_c) of a coil section and the transient azimuthal current in that section. Such a comparison is shown in figure 5 for disks 5, 6, and 7. The critical current in disks 6 and 7 is initially the same since these are symmetric disks in a 12 disk coil. The critical currents are all very high compared to the operating current. For each disk, the critical current is initially constant until the start of the broad increase in the azimuthal current. At that point in time, there is heating and a temperature increase, not shown here, and while the critical current does decrease in time, it remains relatively high compared to the azimuthal current. Within the sharp current spike, however, there is a rapid decrease of the critical current below the azimuthal current, corresponding to a quench. It is interesting to note that quench only occurs here within the sharp current spikes. For the initial disks that go normal in a quench, the maximum amplitude of the current spike is less than the critical current of the associated disk, but as the quench progresses through the coil, the current spikes can equal and exceed the critical current of the associated disks.

Figures 4 and 5 show the relation between currents in adjacent coil sections in the axial direction in successive disks. Returning to figure 3, the relation between currents in adjacent coil sections in the radial direction also can be seen. The traces in figure 3 show the inductive response to a peak current in one section which is seen as resulting in fluctuations in current in the two subsequent sections. This effect

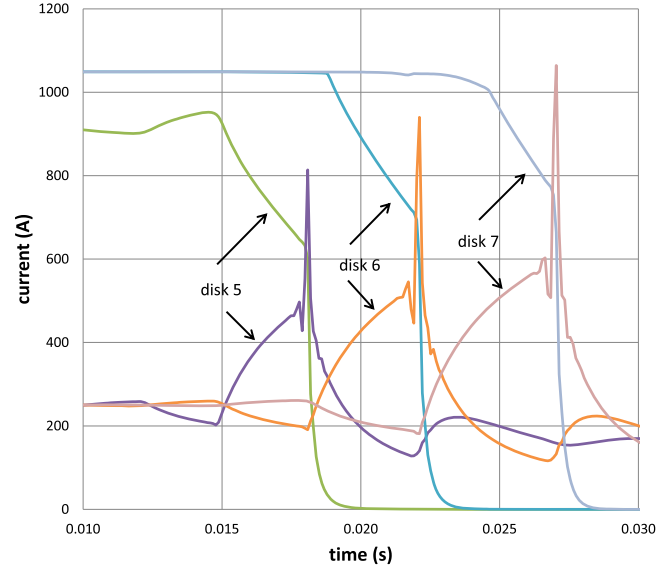


Figure 5. Relation of inductive transient currents (lower traces) and critical current (upper traces) in disks 5, 6, and 7 of coil A during quench for R_s 1.0 $m\Omega\text{ cm}^2$, showing the relative magnitude of the critical current and current transient peaks.

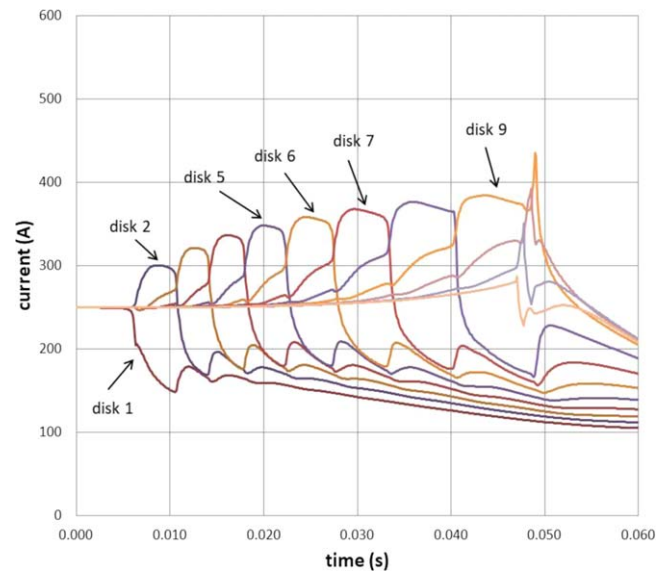


Figure 6. Quench transient currents in test coil A as a function of time at a fixed radius within the winding depth for R_s 50.0 $m\Omega\text{ cm}^2$, showing greatly reduced transient current amplitudes at increased R_s .

results in a small oscillation in current in each section before the peak current in that section. The same oscillations before the peak in current can be seen in the traces in figures 4 and 5, and therefore these oscillations are tied to the radial quench propagation.

All of the quench transients shown so far are for the case of contact resistance R_s 1.0 $m\Omega\text{ cm}^2$. As shown in [5], quench propagation in small coils can persist to quite high values of R_s . Calculated quench transient currents in coil A with R_s 50 $m\Omega\text{ cm}^2$ are shown in figure 6. As described in [5], at increased values of R_s the very nature of quench propagation

changes from sharp spike inductive behavior to a surge in low amplitude azimuthal current. As in the case of figure 5, disk 1 goes normal as indicated by the reduction in current, disk 2 increases in current modestly for a period of time, subsequently quenches, and the pattern is followed through the coil. In this case, however, the quench transient current has only a broad lower peak, as seen for disk 7 in figure 6, and the sharp current spike characteristic of low R_s is not present. The relation of disks 5, 6, and 7 relative to the critical current is again shown in figure 7. In this case, the initial rise in azimuthal current is associated with an initial small decrease in critical current. The broad flat maximum in azimuthal current is accompanied by a steady reduction in critical current until I_c is reduced below the azimuthal current. At that point, rapid quench and reduction of the azimuthal current occurs. In this case, there is relatively rapid quench propagation over the full length of the coil, and yet the magnitude of the transient current is far below the critical current and is limited to moderate values above the initial operating current. The nature of the quench transients is therefore seen to depend importantly on the contact resistance, and it is natural to make a detailed study of this dependence.

The analytical results for the quench transient currents, seen in the preceding figures and in the following parameter study, raise many questions. While fast quench in large NI coils has been observed, there is as yet no direct evidence of the current spikes as shown in the analysis. Further, a major part of the amplitude of the transient at low contact resistance is in the top portion spike of short duration. The analysis does not include eddy current effects in the copper stabilizer which might act to dampen fast current changes. The analysis also does not include a.c. loss effects in the conductor which could possibly result in decreased amplitude of the transients. When first observed in analysis, the full potential impact of quench transient currents was not clear [5]. Reports of recent damage to NI coils associated with quench have put a new emphasis on the importance of the transient currents. An initial understanding of transient currents is important to obtain even if further effects remain to be included.

5. Quench transient currents in test coils

Quench transient currents can conceivably result in coil damage. Therefore, it is important to quantify the quench current amplitude and look for design procedures and parameters that can reduce or minimize the quench transients. Quench transient currents are calculated in the following for the set of coils 1–5 with parameters given in tables 1 and 2. It is important to understand quench transients not only in small coils, but in larger coils as well that will be characteristic of future high field magnets. A set of relatively thin test coils is selected for analysis. There are aspects of coil design and performance that depend on coil diameter, for example the resistance between turns for a constant contact resistance. Thin coils of increasing diameter are selected to study the influence of coil diameter on performance.

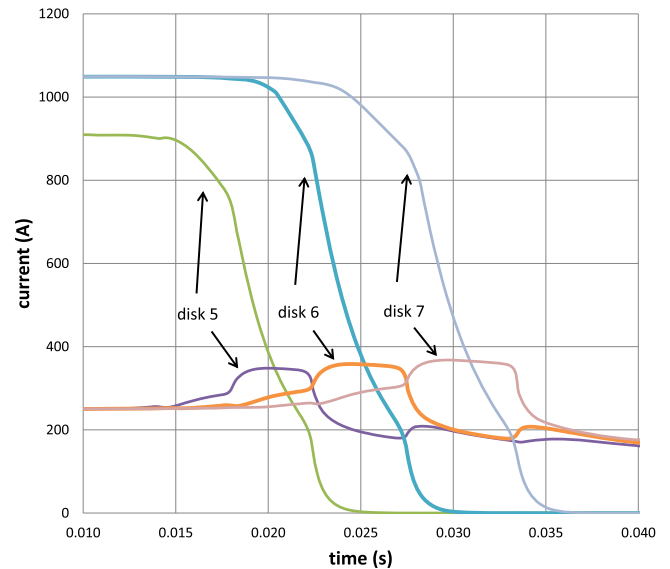


Figure 7. Relation of quench transient currents (lower traces) and critical current (upper traces) in disks 5, 6, and 7 of coil A during quench for R_s 50.0 $m\Omega\text{ cm}^2$, showing relative magnitude of critical current and current transient peaks.

The test coils are intended to display the conditions in the center region of larger, longer coils in high field magnets. But the problem of modeling the central region of a long coil with a shorter coil of finite length is not exact. Although the test coils 1–5 have the same current density, the size difference of the coils results in a small difference in field and critical current. More importantly, as was seen above, the amplitude of the transient current starts low at the end of a coil and increases as the quench progresses. The present test coils were chosen to have 20 disks with the intention that they would be sufficiently long to display behaviors characteristic of yet longer coils.

The conductor selected is a something of a standard with 40 μm total copper thickness and 50 μm Hastelloy core thickness. The influence of variations in the thickness of the copper is not considered in the study. Reduced thickness of copper, with higher current densities in the copper are known to result in faster quench propagation velocities [5]. As seen in table 2, the coil windings include a 10 μm thick steel co-wind. The influence of greatly increased thickness of steel co-wind is also not examined in the study but the resulting lower current density and higher heat capacity is expected to have a limiting effect of quench propagation behavior. A detailed stress analysis design of the test coils is not provided and stress design is not part of this study. A simple estimate shows that the co-wind thickness included here is itself not sufficient to keep the hoop direction strain within practical design limits. A high field coil design can include, in addition, a significant thickness of over-banding reinforcement, which is the assumption here. An alternative is to include a significant quantity of thick co-wind.

The principle parameters of the study, in addition to the coil parameters in the tables, are the contact resistance and the critical current. The influence of the contact resistance on quench propagation was studied when the occurrence of

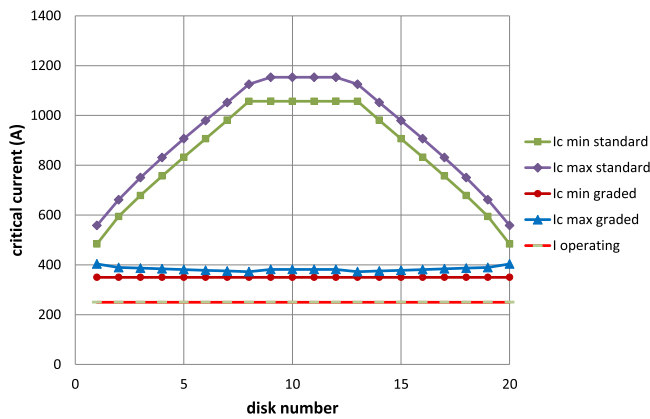


Figure 8. Critical current map through test coil 5 by disk, giving minimum and maximum I_c along the coil by disk, for standard and ideal graded critical current. For standard I_c conductor, the typical large margin above the operating current is seen toward the midplane of the coil where the field orientation angle is low. For ideal graded critical current, the margin is uniform by construction.

quench transient currents was first realized [5]. Here, the focus is on the influence of the contact resistance on the transient current amplitude in addition to the influence on quench propagation. In various preliminary studies, the relation of the critical current magnitude to the amplitude of the transient currents has been noted. Here, two cases are examined for the critical current. In the first case, typical moderate properties for SuperPower REBCO conductor are assumed [22]. The test coils are relatively short inner coils with a long outer coil and as a result the radial fields at the ends are relatively low, such that there is no need for multi-width design or special conductors at the coil ends. The coils are relatively thin, but still there is a variation of field and therefore critical current through the thickness of the coil. As an example, the resulting minimum and maximum of critical current is shown by disk along coil 5 in the upper curves of figure 8. The relatively flat region at the center disks is a result of the decision to limit the calculated critical current at field orientation angles of less than 1° , in recognition of the difficulty of measuring and defining I_c for very low field angles.

The second case examined for critical current is a distribution of critical current within the coil called ideal grading. Grading is the selective placement of reduced critical current tape in the windings. In practice, conductors may be selected from the range of critical current available in a typical production batch, or conductors could be produced with a range of reduced critical current. Also, methods have begun to be explored for the controlled reduction of critical current from production tapes. Here, the engineering methods to obtain graded reduced critical current conductors are not addressed. Rather, as an exercise to determine the effect of going to a theoretical limit, an ideal distribution of critical current is assumed in which the minimum I_c in every disk is set at 350 A, compared to the operating current of 250 A. Again, due to the variation of field within a disk, there is a range of I_c within each disk as shown in the lower curves of figure 8. As seen in the figure, for both cases the variation in the critical current within a disk is small compared to the

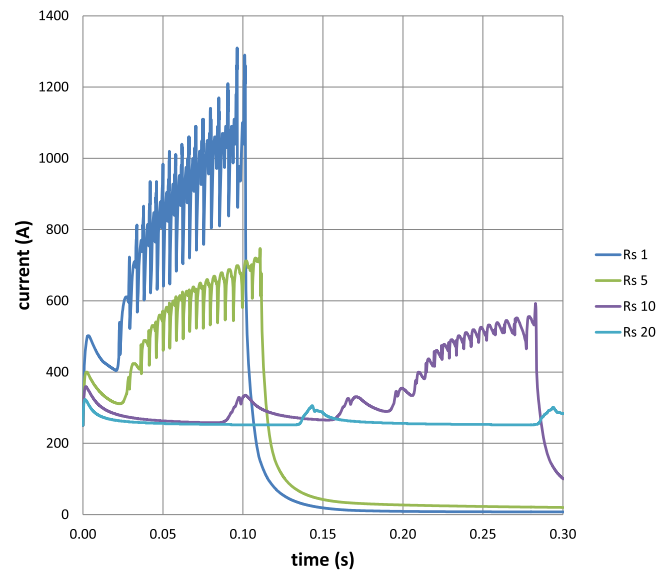


Figure 9. Quench transient current I_{max} during quench in coil 2 with standard I_c showing decreasing transient amplitude with increasing contact resistance R_s to the point of limited quench propagation at R_s 20 $m\Omega\text{ cm}^2$.

absolute value, and the critical current for the case of ideal grading is quite significantly reduced below that for standard production conductor.

Finally, an important result of the study is to show that the size of the test coils, the average radius of the windings, is a significant parameter for the determination of quench transient current and quench propagation in coils with low resistance between turns.

As has been seen in figures 2–7, quench moves along a coil in a sequence of transient current spikes from one disk to the next that have both axial and radial distribution. In order to simplify the presentation of the transient currents, the concept of the maximum azimuthal current $I_{max}(t)$ in a coil at a given time is introduced and used in the following figures. I_{max} is simply the maximum current at a given time anywhere within the coil, but because of the very regular progression of quench, the quantity $I_{max}(t)$ tracks the progress of quench through the coil.

Quench transient currents are first examined for the case of standard production critical current in coils 2–5 of increasing size. The quench transient current in time, as represented by I_{max} , is shown in figure 9 for coil 2 over a range of contact resistance R_s . As R_s increases, the transient currents are reduced in magnitude and become less sharp. For R_s 10 $m\Omega\text{ cm}^2$, the onset of quench propagation is seen to be significantly delayed, but to eventually occur. Figure 10 shows the transients for the next larger coil 3. The transient current characteristics are similar, except now the range of propagation extends to higher values of R_s . For low values of R_s , the maximum amplitudes of the transient currents are similar to those in coil 2. The transient currents for the next larger coils 4 and 5 are shown in figures 11–12, respectively. In each case, at low R_s the maximum values of the transients are similar to those observed in smaller coils, and in each

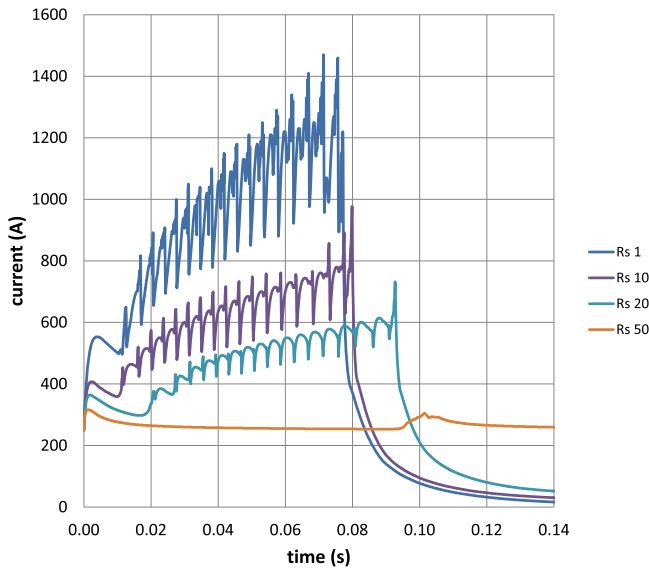


Figure 10. Quench transient current I_{max} during quench in coil 3 with standard I_c showing decreasing transient amplitude with increasing contact resistance R_s to the point of limited quench propagation at R_s 50 $m\Omega\ cm^2$.

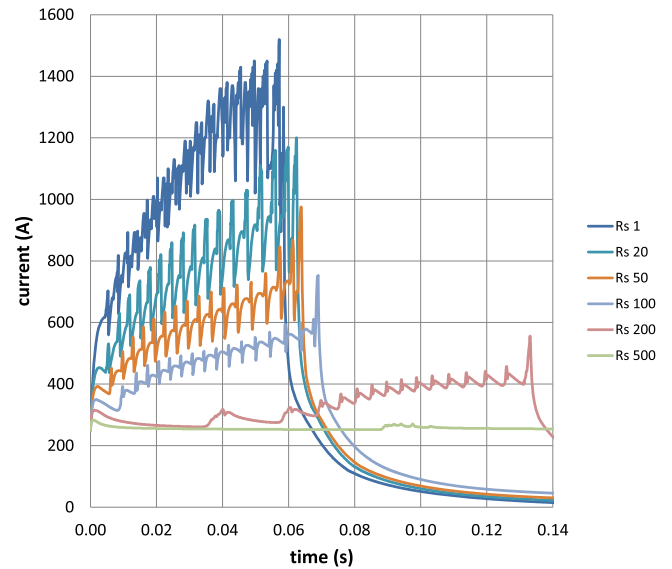


Figure 12. Quench transient current I_{max} during quench in coil 5 with standard I_c showing decreasing transient amplitude with increasing contact resistance R_s to the point of limited quench propagation at R_s 500 $m\Omega\ cm^2$.

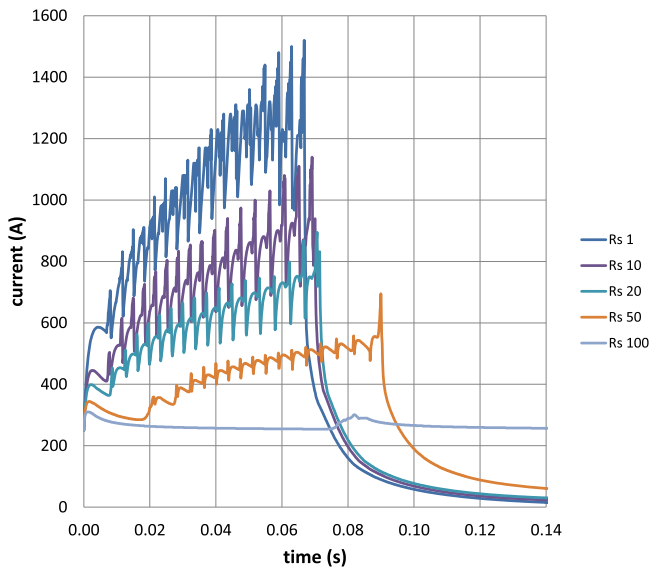


Figure 11. Quench transient current I_{max} during quench in coil 4 with standard I_c showing decreasing transient amplitude with increasing contact resistance R_s to the point of limited quench propagation at R_s 100 $m\Omega\ cm^2$.

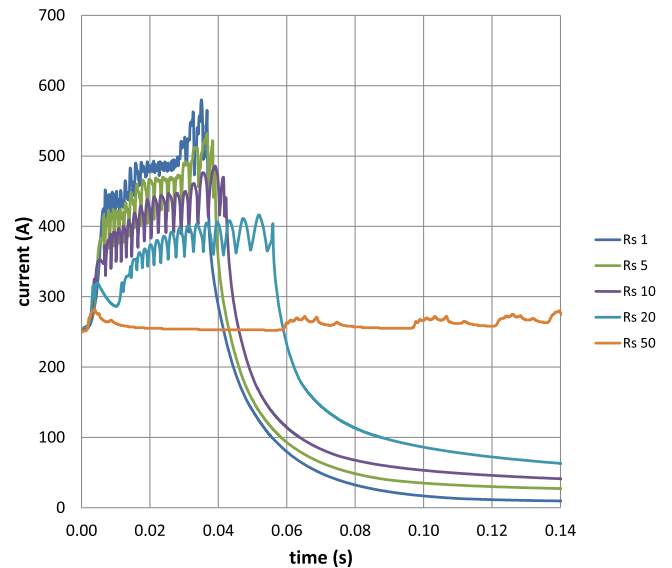


Figure 13. Quench transient current I_{max} during quench in coil 2 with ideal graded I_c showing lower and decreasing transient amplitude with increasing contact resistance R_s to the point of limited quench propagation at R_s 50 $m\Omega\ cm^2$.

case, with increasing size of coil, the propagation of quench extends to yet higher values of contact resistance.

For the case of ideal graded critical current in coils 2–5, the results are similar but with important differences, as seen in figures 13–16. At low values of contact resistance R_s , the quench transient currents are significantly reduced, but not as low as might be expected given the difference in critical current shown in figure 8. For high values of R_s , for each coil size, quench propagation persists to higher values of R_s for the case of ideal graded I_c than for the case of standard production I_c . This is somewhat unexpected. One explanation is that at high values of R_s , where quench propagation is already

diminished, the higher values of I_c in standard production conductor tend to inhibit quench propagation in comparison with the lower values of I_c in the graded conductor.

During the course of a quench, $I_{max}(t)$ generally increases until, toward the end of the quench, toward the end of the coil, $I_{max}(t)$ reaches a peak value for that quench. The peak value of $I_{max}(t)$, for the coil size and parameters of that quench, is tabulated as the quench maximum transient current I_{QM} . The results of the test coil parameter study are presented in terms of the quench maximum transient current I_{QM} as a function of the contact resistance in figure 17. I_{QM} is given for each of coils 1–5, for both standard and ideal graded critical

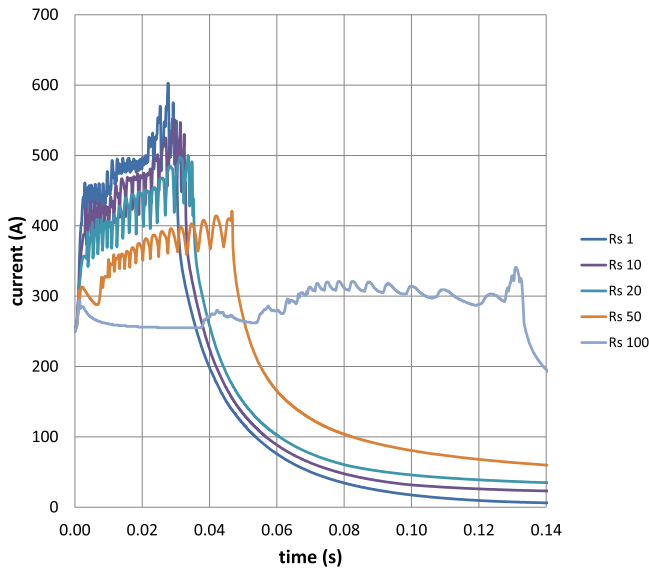


Figure 14. Quench transient current I_{max} during quench in coil 3 with ideal graded I_c showing lower and decreasing transient amplitude with increasing contact resistance R_s to the point of limited quench propagation at R_s 100 $m\Omega\text{ cm}^2$.

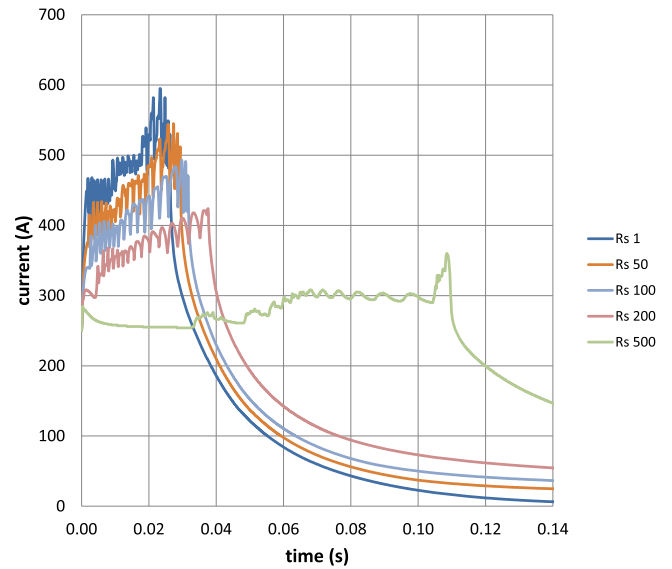


Figure 16. Quench transient current I_{max} during quench in coil 5 with ideal graded I_c showing lower and decreasing transient amplitude with increasing contact resistance R_s to the point of limited quench propagation at R_s 500 $m\Omega\text{ cm}^2$.

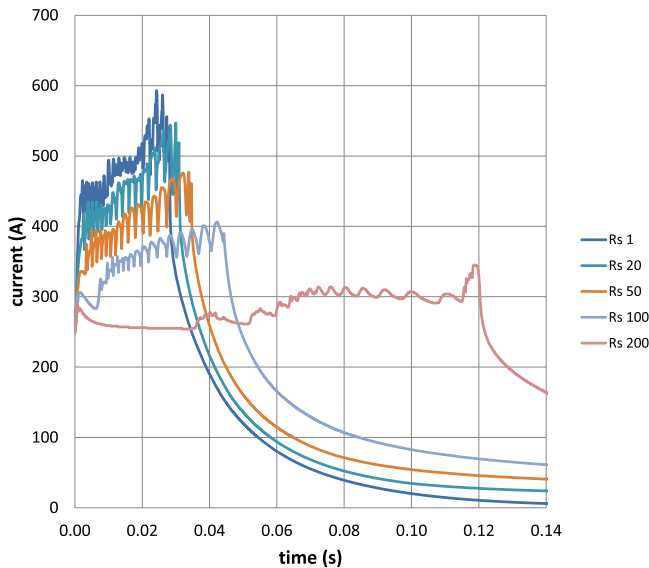


Figure 15. Quench transient current I_{max} during quench in coil 4 with ideal graded I_c showing lower and decreasing transient amplitude with increasing contact resistance R_s to the point of limited quench propagation at R_s 200 $m\Omega\text{ cm}^2$.

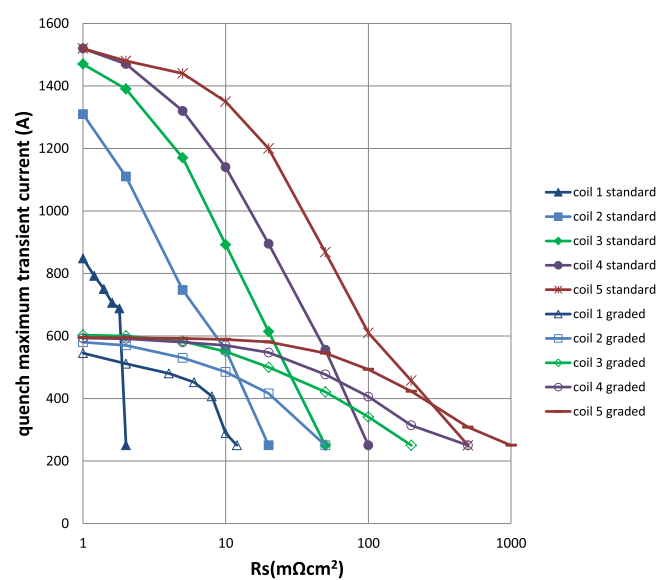


Figure 17. Quench maximum transient current I_{QM} during quench in test coils 1–5 versus contact resistance R_s for standard and ideal graded I_c , showing the decrease of I_{QM} with increasing R_s generally, the increase of the envelop of I_{QM} with increasing coil size from coil 1 to 5, and the significant reduction in I_{QM} resulting from the assumed ideal grading of I_c . The reduction of I_{QM} to the operating current of 250 A represents the effective quench propagation limit QPL.

current. For standard critical current, at low R_s of 1 $m\Omega\text{ cm}^2$, the maximum transient currents during a quench are seen to increase with coil size to a limiting value. Not shown is that for smaller coils yet and lower values of R_s , the value of I_{QM} continues to increase to the same high limit. For increased R_s , the high values of transient current are eventually reduced and eliminated. As the size of the coil increases, the characteristic curve for the reduction of I_{QM} is shifted to higher values of R_s . In the case of ideal graded I_c , at low values of R_s there is significant reduction of maximum transient current I_{QM} below the values observed for standard critical current, but this reduction is for ideal grading which is a rather extreme

reduction in critical current, and even in this case the remaining value of I_{QM} may be large for mechanical stress considerations. For ideal graded I_c , the falloff of I_{QM} at high R_s is comparable to the case with standard I_c , however the falloff is noticeably more gradual. This could be advantageous in defining a regime with low I_{QM} but that still guarantees adequate quench propagation.

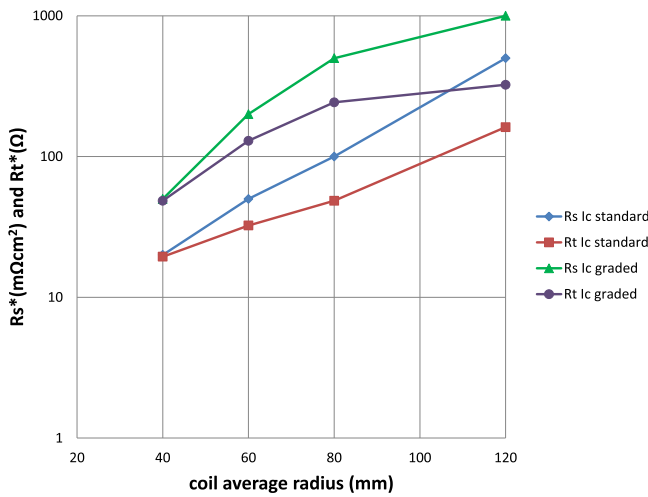


Figure 18. The values of contact resistance R_s^* and turn resistance R_t^* are shown at the quench propagation limit QPL as a function of coil average radius for standard and ideal graded critical current as obtained for test coils 2–5. Importantly, at the quench propagation limit the turn resistance generally increases with coil size.

In the construction of figure 17, a concept of quench propagation limit (QPL) is introduced. At very high values of R_s , while a particular calculation may show small residual current spikes as initial disks quench, if it is judged that no useful quench propagation occurs, the value of R_s is considered to exceed the QPL. In that case, instead of recording the ripple increase in I_{QM} in figure 17, the convention was to record the initial operating current, a value of 250 A, indicating no transient current. With this convention, the point at which the I_{QM} values for each coil are reduced to 250 A is the QPL for that coil. Defined in this way, the QPL gives a relation between the size of a coil and the value of R_s^* at the QPL. If the size of the coil is defined by the average radius, then the value of R_s defines a value of the turn resistance R_t at that radius. The result is a relation between the average coil radius and the value of R_s^* and R_t^* at the QPL, as shown in figure 18 for both the case of standard production critical current and the case of ideal grading. It is seen that the resistance between turns is not a constant at the QPL. If indeed quench propagation in NI coils is an inductive process, then it might be expected that the inductance of a coil, and therefore the size, is involved in the conditions for quench propagation, and not just the resistance.

6. Spatial and temporal distribution of quench transient currents

Transient current behavior is studied, importantly, as input to coil stress analysis. The maximum current I_{max} , defined above, is used as a simple measure to display trends and dependence on design parameters of the transient current magnitude. For stress analysis, a more detailed description of the transients is needed. It is emphasized that the transients have a distribution in space and time in each disk. As an example, in figures 19(a)–(d) are shown the transients in disk

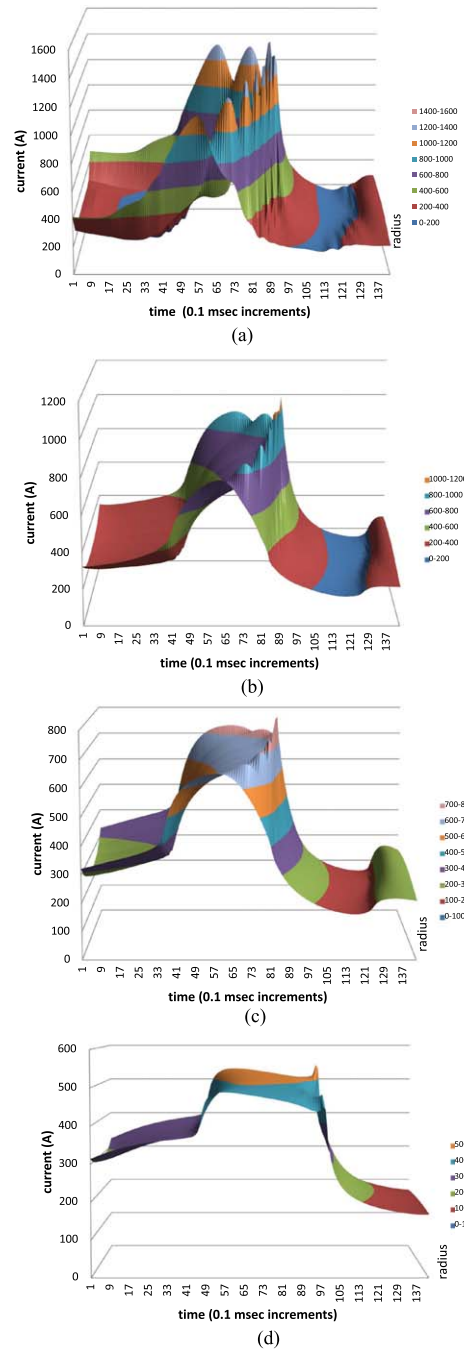


Figure 19. Quench transient currents in coil 4, disk 16, with standard critical current over a 14 ms time interval showing a decrease in the magnitude and complexity of the transient currents with increased contact resistance for: (a) 1.0, (b) 10.0, (c) 20.0 and (d) 50.0 $m\Omega\ cm^2$.

16 of coil 4 as a function of time through the radial depth of the coil for a range of R_s and standard critical current. In figure 19(a) at low R_s , there is considerable variation of the transient current amplitude through the disk in space and time, and a detailed time dependent stress analysis may be required. As the value of R_s increases in figures 19(b)–(d), the transient current becomes more smooth and regular through the depth of the coil and a more simple stress analysis may be adequate.

7. Resistive insulation (RI) coil technology

Two very important aspects of NI coil technology are (1) the increased mechanical properties as a result of removing soft insulation, and (2) rapid quench propagation as the mechanism for quench protection. The results here emphasize the fact that rapid quench propagation extends to very high values of R_s , especially for coils of increasing size. The results suggest a variant of NI technology with controlled high values of R_s . Stability will be decreased, but stability is much decreased in insulated coils in comparison to NI coils. The contact resistance R_s of so called metallic insulation is now known to be dominated by actual surface oxide insulation. It is possible to imagine a coil technology based on surface insulations including oxides and other materials to give high and controlled finite values of the surface resistivity R_s . For coil performance, it is the value of R_s that is important and not the exact type of insulation. In recognition, a general term for a coil technology formulated around the value of R_s would be resistive insulation (RI) coils.

8. Quench at or above the QPL

At this point in the development of the technology, it is common to characterize REBCO coils as either NI or insulated. Behind these labels is the important difference in quench behavior, namely that NI coils display fast quench propagation while insulated coils do not. In light of the present work, there is a wide range of possible contact resistance in a coil, and the difference in quench behavior may be directly correlated with the value of the contact resistance. For R_s below the QPL, there is effective quench propagation, while at or above the QPL there is not. Still, at the QPL and even above, there is residual transient current, or bypass current, through the finite value of the contact resistance. This residual bypass current does provide, in principle, additional time for active protection methods and, in principle, could lead to a reduction in the amount of stabilizer copper required for a coil somewhat above the QPL in comparison to a fully insulated coil. As indicated above in the definition of screening currents and transient currents, the distribution of current across the conductor is not included in the present work. While the conditions at or above the QPL could be studied further by the methods used here, a more complete understanding will be obtained by including the distribution of currents within the conductor in the analysis.

9. Summary and conclusions

Experience has shown that NI coils are not immune to mechanical damage during operation and quench. Earlier analysis had shown that quench in NI coils is characterized by large transient currents, and therefore large transient forces. One is motivated to examine quench transients in NI coils for the purpose of characterizing the transients for stress analysis. One is further motivated to examine ways to eliminate or diminish the effects of quench transients in NI coil performance.

The characteristics of quench transient currents are examined over a range of contact resistance R_s . At low R_s , the transients are very fast, of short duration, with high sharp peaks, are localized in the winding depth, and are distributed in time within a disk in a coil. At larger R_s , the transients are lower in amplitude, of longer duration in time, and more uniformly distributed through the radial depth of a coil. At low R_s , a true transient stress analysis would appear to be required. At high R_s , a static stress analysis becomes more applicable.

In order to examine the possibilities for reducing or eliminating the quench current transients, a parameter study was made with a series of test coils. The parameters include contact resistance, critical current, and also coil size. The contact resistance was varied from 1 to 1000 m Ω cm². The critical current options included either standard REBCO properties, or a heavily limited critical current called ideal grading. The coils sizes spanned the range that would be involved in a small bore high field magnet, from the smaller inner coil to the larger outer coil.

At low values of R_s , especially for standard critical current, quench transient currents are very large in comparison with the operating current. A major decrease in critical current with the assumed ideal grading does result in a significant decrease in transient amplitude, but not as large a decrease as might be expected, and not enough of a decrease to eliminate the mechanical problem posed by the transients. As R_s is increased, at first quench propagation remains fast and robust until finally, at R_s much larger than is typical for NI coils, quench propagation is diminished and finally ceases at the QPL. And as R_s is increased, there is reduction in transient current amplitude for both standard and ideal graded critical current, gradually at first, until near the QPL the transients are significantly reduced. Importantly, the value of R_s at which the current transient amplitude is reduced depends directly on the coil diameter.

The use of increased contact resistance is identified as a way to decrease the quench current transient amplitude, and with it the associated mechanical forces. An increase in R_s in the range below but approaching the QPL would put the coil in a regime where rapid quench propagation was still operative. An increase in R_s combined with a reduction in critical current, such as ideal graded conductor, reduces the steepness of the QPL boundary and may provide wider design tolerance in the engineering of the contact resistance value. More broadly, there is the open possibility that contact resistance R_s near but above the QPL, together with active protection methods, may offer protection advantages over that of a fully insulated system. The manner in which the increased contact resistance would be obtained is expected to be an extension of present work on surface coating and surface treatment of steel co-wind. The resulting coil technology would appropriately be called RI coils.

ORCID iDs

W Denis Markiewicz  <https://orcid.org/0000-0002-6888-0150>

References

- [1] Hahn S, Park D K, Bascunan J and Iwasa Y 2011 HTS pancake coils without turn-to-turn insulation *IEEE Trans. Appl. Supercond.* **21** 1592–4
- [2] Choi S, Jo H C, Hwang Y J, Hahn S and Ko T K 2012 A study on the no-insulation winding method of the HTS coil *IEEE Trans. Appl. Supercond.* **22** 4904004
- [3] Lecrevisse T and Iwasa Y 2016 A (RE)BCO pancake winding with metal-as-insulation *IEEE Trans. Appl. Supercond.* **26** 4700405
- [4] Song J B, Hahn S, Lecrevisse T, Voccio J, Bascunan J and Iwasa Y 2015 Over-current quench test and self-protection behavior of a 7 T/78 mm multi-width no-insulation REBCO magnet at 4.2 K *Supercond. Sci. Technol.* **28** 114001
- [5] Markiewicz W D, Jaroszynski J J, Abraimov D V, Joyner R E and Khan A 2016 Quench analysis of pancake wound REBCO coils with low resistance between turns *Supercond. Sci. Technol.* **29** 025001
- [6] Yoon S, Kim J, Cheon K, Lee H, Hahn S and Moon S-H 2016 26 T 35 mm all-GdBa₃Cu₃7-x multi-width no-insulation superconducting magnet *Supercond. Sci. Technol.* **29** 04LT04
- [7] Bascunan J, Hahn S, Lecrevisse T, Song J, Miyagi D and Iwasa Y 2016 An 800-MHz all-REBCO insert for the 1.3-GHz LTS/HTS NMR magnet program—a progress report *IEEE Trans. Appl. Supercond.* **26** 4300205
- [8] Michael P, Park D, Choi Y H, Lee J, Li Y, Bascunan J, Noguchi S, Hahn S and Iwasa Y 2019 Assembly and test of a 3-nested coil 800MHz REBCO Insert (H800) for the MIT 1.3GHz LTS/HTS NMR magnet *IEEE Trans. Appl. Supercond.* **29** 4300706
- [9] Hahn S, Kim K L, Kim K, Hu X, Painter T, Dixon I, Kim S, Bhattarai K R, Noguchi S, Jaroszynski J and Larbalestier D C 2019 45.5-tesla direct-current magnetic field generated with a high-temperature superconducting magnet *Nature* **570** 496–9
- [10] Noguchi S 2019 Electromagnetic, thermal, and mechanical quench simulation of NI REBCO pancake coils for high magnetic field generation *IEEE Trans. Appl. Supercond.* **29** 4602607
- [11] Noguchi S, Park D, Choi Y, Lee J, Li Y, Michael P C, Bascunan J, Hahn S and Iwasa Y 2019 Quench analysis of the MIT 1.3 GHz LTS/HTS NMR magnet *IEEE Trans. Appl. Supercond.* **29** 4301005
- [12] Yang D G, Kim K L, Choi Y H, Kwon O J, Park Y J and Lee H G 2013 Screening current induced field in non-insulated GdBCO pancake coil *Supercond. Sci. Technol.* **26** 105025
- [13] Maeda H and Yanagisawa Y 2014 Recent developments in high temperature superconducting magnet technology (review) *IEEE Trans. Appl. Supercond.* **24** 4602412
- [14] Ma D X, Zhang Z Y, Matsumoto S, Teranishi R and Kiyoshi T 2013 Degradation of REBCO conductors caused by the screening current *Supercond. Sci. Technol.* **26** 105018
- [15] Bhattarai K R, Kim K L, Kim S, Lee S G and Hahn S 2017 Quench analysis of a multiwidth no insulation 7-T 78-mm REBCO magnet *IEEE Trans. Appl. Supercond.* **27** 4603505
- [16] Wang T, Noguchi S, Wang W, Arakawa I, Minami K, Ishiyama A, Hahn S and Iwasa Y 2015 Analysis of transient behaviors of no-insulation REBCO pancake coils during sudden discharging and overcurrent *IEEE Trans. Appl. Supercond.* **25** 4603409
- [17] Lu J, Goddard R, Han K and Hahn S 2017 Contact resistance between two REBCO tapes under load and load cycles *Supercond. Sci. Technol.* **30** 045005
- [18] Bonura M, Barth C, Joudrier A, Troitin J F, Fete A and Senatore C 2019 Systematic study of the contact resistance between REBCO tapes: pressure dependence in the case of no-insulation, metal co-wind and metal-insulation *IEEE Trans. Appl. Supercond.* **29** 48511141
- [19] Lecrevisse T, Badel A, Benkel T, Chaud X, Fazilleau P and Tixador P 2018 Metal-as-insulation variant on no-insulation HTS winding technique: pancake tests under high Background magnetic field and high current at 4.2 K *Supercond. Sci. Technol.* **31** 055008
- [20] Lu J, Levitan J, McRae D and Walsh R 2018 Contact resistance between two REBCO tapes: the effects of cyclic loading and surface coating *Supercond. Sci. Technol.* **31** 085006
- [21] Lu J, Levitan J, Radcliff K, Kim K L, Xin Y, Goddard R and Bai H 2018 Control of contact resistivity between REBCO tapes *Applied Superconductivity Conference (Seattle, WA)*
- [22] Xu A, Jaroszynski J J, Kametani F, Chen Z, Larbalestier D C, Vioicjkov Y L, Chen Y, Xie Y and Selvamanickam V 2010 Angular dependence of J_c of YBCO coated conductors at low temperature and very high magnetic fields *Supercond. Sci. Technol.* **23** 014003